Proteome–Metabolome Profiling of Ovarian Cancer Ascites Reveals Novel Components Involved in Intercellular Communication*[S]

Victoria O. Shender‡§¶, Marat S. Pavlyukov‡¶, Rustam H. Ziganshin‡, Georgij P. Arapidi‡‖, Sergey I. Kovalchuk‡, Nikolay A. Anikanov‡, Ilya A. Altukhov‖, Dmitry G. Alexeev‖**, Ivan O. Butenko**, Alexey L. Shavarda‡‡§§, Elena B. Khomyakova**, Evgeniy Evtushenko¶¶, Lev A. Ashrafyan‖‖, Irina B. Antonova‖‖, Igor N. Kuznetcov‖‖, Alexey Yu. Gorbachev**, Mikhail I. Shakhparonov‡, and Vadim M. Govorun‡**[a]**

Ovarian cancer ascites is a native medium for cancer cells that allows investigation of their secretome in a natural environment. This medium is of interest as a promising source of potential biomarkers, and also as a medium for cell–cell communication. The aim of this study was to elucidate specific features of the malignant ascites metabolome and proteome. In order to omit components of the systemic response to ascites formation, we compared malignant ascites with cirrhosis ascites. Metabolome analysis revealed 41 components that differed significantly between malignant and cirrhosis ascites. Most of the identified cancer-specific metabolites are known to be important signaling molecules. Proteomic analysis identified 2096 and 1855 proteins in the ovarian cancer and cirrhosis ascites, respectively; 424 proteins were specific for the malignant ascites. Functional analysis of the proteome demonstrated that the major differences between cirrhosis and malignant ascites were observed for the cluster of spliceosomal proteins. Additionally, we demonstrate that several splicing RNAs were exclusively detected in malignant ascites, where they probably existed within protein complexes. This result was confirmed *in vitro* using an ovarian cancer cell line. Identification of spliceosomal proteins and RNAs in an extracellular medium is of particular interest; the finding suggests that they might play a role in the communication between cancer cells. In addition, malignant ascites contains a high number of exosomes that are known to play an important role in signal transduction. Thus our study reveals the specific features of malignant ascites that are associated with its function as a medium of intercellular communication. ***Molecular & Cellular Proteomics 13: 10.1074/mcp.M114.041194, 3558–3571, 2014.***

From the ‡Shemyakin-Ovchinnikov Institute of Bioorganic Chemistry, Miklukho-Maklaya str. 16/10, Moscow 117997, Russian Federation; ‖Moscow Institute of Physics and Technology, Institutskiy pereulok 9, Dolgoprudny 141700, Russian Federation; **Research Institute of Physical Chemical Medicine, Malaya Pirogovskaya str., 1a, Moscow 119435, Russian Federation; ‡‡Research Resource Center molecular and Cell Technologies, Saint-Petersburg State University, Universitetskaya nab. 7-9, Saint-Petersburg 199034, Russian Federation; §§Analytical Phytochemistry Laboratory, Komarov Botanical Institute, Prof. Popov Street 2, Saint-Petersburg 197376, Russia; ¶¶Faculty of Chemistry, Lomonosov Moscow State University, Leninskiye Gory 1-3, Moscow 119991, Russian Federation; ‖‖Russian Scientific Center of Roentgenoradiology, Profsoyuznaya str. 86, Moscow 117997, Russian Federation; [a]Kazan Federal University, Kremlyovskaya str. 18, Kazan 420008, Russian Federation

Received May 13, 2014, and in revised form, August 28, 2014
Published, MCP Papers in Press, September 30, 2014, DOI 10.1074/mcp.M114.041194

Author contributions: V.O.S., M.S.P., R.H.Z., M.I.S., and V.M.G. designed research; V.O.S., M.S.P., G.P.A., S.I.K., N.A.A., A.L.S., E.K., E.E., and A.Y.G. performed research; V.O.S., M.S.P., G.P.A., S.I.K., N.A.A., I.A.A., D.G.A., I.O.B., A.L.S., E.K., and E.E. analyzed data; V.O.S., M.S.P., R.H.Z., and G.P.A. wrote the paper; L.A.A., I.B.A., and I.N.K. performed biological sample collection.

Ovarian cancer is the sixth most frequently occurring cancer among the gynecological cancers and accounts for about 5% of all new female cancer cases according to the 2012 data (World Health Organization International Agency for Research on Cancer www.globocan.iarc.fr). Epithelial ovarian cancer registered in 90% of ovarian cancer cases. The rate of mortality from ovarian cancer holds first place among the other gynecological cancers, largely because of the asymptomatic progression of the disease, especially at its early stages, and a lack of adequate screening tests, which leads to late detection, typically only after the cancer has spread to adjacent structures. In such a case, the five-year survival rate is only 25% to 40%, whereas it can be as high as 90% if the cancer is diagnosed early. Unfortunately, ovarian cancer is diagnosed early in less than 20% of the total number of cases (International Agency for Research on Cancer). The main methods for primary diagnostics include transvaginal ultrasound and blood biomarker analyses such as with cancer

antigen 125 (CA125),[1] epididymis protein-4 (HE4), and the OVA1 multiparametric (CA125, β2-microglobulin, transferrin, and apolipoprotein A1) tests. The OVA1 test is mainly applied to evaluate the malignancy of a tumor-like pelvic mass, and the other two markers are used to monitor disease progress and estimate treatment efficacy, as they are not highly specific for ovarian cancer and thus produce a high percentage of false-positive results (1). Therefore, the search for specific and sensitive markers for the early diagnosis of ovarian cancer is an urgent problem, although the development of new, efficient methods for treatment of the disease at late stages also remains of critical importance.

One of the symptoms associated with late-stage ovarian cancer is excessive fluid accumulation in the abdominal cavity, known as ascites. Mechanisms of malignant ascites formation involve lymph obstruction, activation of mesothelial cells as a result of the metastatic process, and increased vessel permeability due to the secretion of growth factors (2, 3). Therefore, malignant ascites is enriched by tumor cells and soluble growth factors that may be associated with the processes of invasion and metastasis. Thus, ascites provides a native medium for cancer cells and creates an opportunity to investigate the ovarian cancer cell secretome in its natural environment (as distinct from cancer cell cultures *in vitro*) (2).

Omics studies enable us to understand physiological information at different levels (4–7). Considering the highly diverse features of information obtained from each omics platform, one could expect that combinations of different omics should provide highly comprehensive views on special features of the cancer cell secretome. Studies of ascites with the use of omics technologies could not only help us understand the peculiarities of the vital activity of cancer cells in the organism, but also elaborate new therapeutic methods. However, until now, proteomic studies of ovarian cancer ascites have been exceptionally directed at the search for potential biomarkers of this cancer (3, 8–10). Investigation of ascites is also interesting beyond the protein level. In particular, small molecules—metabolites—are known to be involved in intercellular communication. However, in metabolome studies, to our knowledge, metabolites from ovarian cancer ascites have not been explored at all; only metabolomic analysis of urine and serum has been described in the literature for this type of cancer (11–13).

It is important to note that ascites accumulation can be caused by various pathologies—for example, liver cirrhosis (81% of all cases), heart diseases (2%), tuberculosis (3%), and 10% of all cases associated with malignancy (10%). The most common cancer associated with ascites is ovarian cancer, accounting for 38% of malignant ascites occurring in females (2). In this study, we compared ascites of different etiologies, formed in the course of ovarian cancer and portal alcoholic cirrhosis. Thus, we not only extended our knowledge of the protein composition and filled in gaps regarding the metabolome, but also elucidated specific features of malignant ascites composition.

EXPERIMENTAL PROCEDURES

Patients and Specimens—Ascitic samples from 10 ovarian cancer patients (hereinafter referred to as "malignant ascites") were obtained from the Russian Scientific Center of Roentgenoradiology (Moscow, Russia) and the Blokhin Cancer Research Center of the Russian Academy of Medical Sciences (Moscow, Russia). All patients had been previously treated with chemotherapy. Ascitic samples from five patients with portal alcoholic cirrhosis (hereinafter referred to as "cirrhosis ascites") were obtained from the Central Research Institute of Gastroenterology (Moscow, Russia). Characteristics of the biological material are given in the supplemental "Materials and Methods" section. All diagnoses were confirmed by morphological studies. The study was approved by the ethics committees of the corresponding hospitals, and all the patients gave written informed consent for their participation.

Ascitic Fluid Samples—The ascitic fluids from both groups were taken in standard tubes of 9-ml volume without any filler. The ascitic fluids were centrifuged at 1900 × *g* (3000 rpm) for 15 min at room temperature in order to remove the cells. The samples were stored at −70 °C and transported in liquid nitrogen. Prior to proteomic analysis, the samples were centrifuged at 16,000 × *g* for 30 min to remove the cellular debris.

Comprehensive protein identification was performed for 10 malignant and 5 cirrhosis ascites samples. Proteome analyses of both types of ascites were carried out with and without a protein depletion procedure (Fig. 1*C*). Proteome analysis with combinatorial peptide ligand library (CPLL) treatment was performed using pools of malignant and cirrhosis ascites and carried out in triplicate. Proteome experiments without CPLL treatment were performed on pooled malignant and cirrhosis ascites; in addition, LC-MS/MS analysis was performed for 10 individual malignant samples in a single repeat. Metabolome analysis was performed for seven malignant and four cirrhosis individual ascites samples in triplicate.

Sample Preparation for the Metabolome GC-MS Analysis—100 μl of ascites were aliquoted, and then 300 μl of methanol were added. After 15 s of vortexing, the protein precipitate was pelleted by centrifugation at 16,000 × *g* for 15 min at room temperature. Then 90-μl aliquots were transferred into new tubes, and each sample was lyophilized in a centrifugal vacuum evaporator for 18 h.

Freeze-dried samples were dissolved in 20 μl of pyridine and converted to trimethylsilyl derivatives by the addition of 20 μl of N,O-bis-(trimethylsilyl) trifluoroacetamide containing 1% trimethylchlorosilane. The chemical reaction was induced by heating to 100 °C for 15 min; 0.5 μl of this reaction mixture was injected into the gas chromatograph.

GC-MS and Data Analysis—Silylated samples were analyzed using an HP 6850 gas chromatograph interfaced with an HP 5975C mass selective detector. An HB5-MS capillary column (30 m × 0.25 mm inner diameter; film thickness of 0.25 μm) was used with helium as a carrier gas at a constant rate of 1 ml/min. The temperatures of the injector and MS source were maintained at 320 °C and 230 °C, respectively. The column temperature program consisted of injection at 70 °C with an increase of 6 °C/min up to 320 °C followed by an isothermal hold at 320 °C for 15 min. Tricosane (10 μg) was used as

[1] The abbreviations used are: CA125, cancer antigen 125; HE4, epididymis protein-4; ACN, acetonitrile; CPLL, combinatorial peptide ligand library; GC-MS, gas chromatography–mass spectrometry; GO, Gene Ontology; LC-MS/MS, liquid chromatography–tandem mass spectrometry; snRNA, small nuclear RNA; RNP, ribonucleoprotein complex; miRNA, microRNA; TGM2, transglutaminase 2.

an internal standard for the quantification of analytical results. The samples were analyzed in split mode (split ratio: 1/20). The mass spectrometer was operated in the electron impact mode with an ionization energy of 70 eV. The scan mass range was set from 50 to 1000 Da at 1.27 scans per second.

The data were processed and quantified with the AMDIS software. Compounds were identified through comparison with the chromatographic retention characteristics and mass spectra of authentic standards, reported mass spectra, and the mass spectral library of the GC-MS data system (National Institute of Standards and Technology 2010). The sum of the extracted ion chromatograms of the ions associated with a compound was used for quantification.

Combinatorial Peptide Ligand Library Treatment—Reagent and column preparation, sample binding, and sample washes were carried out according to the manufacturer's protocol (ProteoMiner Protein Enrichment Kit, Bio-Rad). The sorbed proteins were twice eluted with 100 μl of four different solutions: (i) 1 M NaCl, 20 mM HEPES, pH 7.5; (ii) 200 mM glycine-HCl, pH 2.4; (iii) 60% ethylene glycol; and (iv) 13.3% isopropyl alcohol, 7% ACN, 0.1% TFA. The acidic protein fraction was neutralized by the addition of 3 M Tris-HCl immediately after the elution.

All fractions were pooled together and added to a 5-kDa molecular weight cutoff Agilent spin concentrator (Agilent Technologies, Santa Clara, CA) for buffer exchange. The concentration of each sample pool was measured, and then 240 μg of each sample was put into a new microtube, concentrated in a SpeedVac evaporator to 10 μl, and separated via SDS-PAGE.

SDS-PAGE—Biological samples were separated via 9% (w/v) SDS-PAGE (20 cm $\times$ 20 cm) to prefractionate the proteins. Electrophoresis was stopped when the dye front reached 5 cm below the stacking gel. Subsequently, the gel was divided into 12 slices, each slice was subjected to in-gel protein digestion, and extracted peptide samples were analyzed via LC-MS/MS for protein identification.

In-gel Trypsin Digestion of Protein Samples—Gel slices were cut into small (1 mm $\times$ 1 mm) pieces and transferred into sample tubes. Protein disulfide bonds were reduced with 10 mM DTT (in 100 mM ammonium bicarbonate buffer) at 50 °C for 30 min and afterward alkylated with 55 mM iodoacetamide (in 100 mM ammonium bicarbonate buffer) at room temperature for 20 min in the dark. After alkylation, the gel samples were destained with 50% ACN (in 50 mM ammonium bicarbonate buffer) and dehydrated by the addition of 100% ACN. After removal of the 100% ACN, the samples were subjected to in-gel trypsin digestion. The digestion buffer contained 13 ng/μl trypsin (in 50 mM ammonium bicarbonate buffer). The trypsin digestion proceeded overnight at 37 °C. The resulting tryptic peptides were extracted from the gel via the addition of two volumes of 0.5% TFA to the samples (incubation for 1 h) and then two volumes of 50% ACN (incubation for 1 h). Finally, the extracted peptides were dried in vacuum and redissolved in 3% ACN with 0.1% formic acid solution prior to LC-MS/MS analysis.

LC-MS/MS Analysis—Analysis was performed on a TripleTOF 5600+ mass spectrometer with a NanoSpray III ion source (AB Sciex, Framingham, MA) coupled with a NanoLC Ultra 2D+ nano-HPLC system (Eksigent, Dublin, CA). The HPLC system was configured in trap-elute mode. For sample loading buffer and buffer A, a mixture of 98.9% water, 1% methanol, 0.1% formic acid (v/v) was used. Buffer B was 99.9% acetonitrile and 0.1% formic acid (v/v). Samples were loaded on a Chrom XP C18 trap column (3 μm, 120 Å, 350 μm $\times$ 0.5 mm; Eksigent) at a flow rate of 3 μl/min for 10 min and eluted through a 3C18-CL-120 separation column (3 μm, 120 Å, 75 μm $\times$ 150 mm; Eksigent) at a flow rate of 300 nl/min. The gradient was from 5% to 40% buffer B in 90 min followed by 10 min at 95% buffer B and 20 min of reequilibration with 5% buffer B. Between different samples, two blank 45-min runs consisting of 5 to 8 min waves (5% B, 95%, 95%, 5%) were required to wash the system and to prevent carryover.

The information-dependent mass-spectrometer experiment included one survey MS1 scan followed by 50 dependent MS2 scans. MS1 acquisition parameters were as follows: the mass range for MS2 analysis was 300–1250 *m/z*, and the signal accumulation time was 250 ms. Ions for MS2 analysis were selected on the basis of intensity with a threshold of 200 counts per second and a charge state from 2 to 5. MS2 acquisition parameters were as follows: the resolution of the quadrupole was set to UNIT (0.7 Da), the measurement mass range was 200–1800 *m/z*, and the signal accumulation time was 50 ms for each parent ion. Collision-activated dissociation was performed with nitrogen gas with the collision energy ramped from 25 to 55 V within the signal accumulation time of 50 ms. Analyzed parent ions were sent to the dynamic exclusion list for 15 s in order to get an MS2 spectra at the chromatographic peak apex.

β-Galactosidase tryptic solution (20 fmol) was run with a 15-min gradient (5% to 25% buffer B) every two samples and between sample sets to calibrate the mass spectrometer and to control the overall system performance, stability, and reproducibility.

LC-MS/MS Data Analysis—Raw LC-MS/MS data were converted to .mgf peaklists with ProteinPilot (version 4.5). For this procedure we ran ProteinPilot in identification mode with the following parameters: Cys alkylation by iodoacetamide, trypsin digestion, TripleTOF 5600 instrument, and thorough I.D. search with a detected protein threshold of 95.0% against the UniProt human protein knowledgebase (version 2013 03, with 150,600 entries). For thorough protein identification, the generated peak lists were searched with the MASCOT (version 2.2.07) and X! Tandem (CYCLONE, 2013.2.01) search engines against the UniProt human protein knowledgebase (version 2013 03) with the concatenated reverse decoy dataset (with 301,200 entries in all). The precursor and fragment mass tolerance were set at 20 ppm and 0.04 Da, respectively. Database-searching parameters included the following: tryptic digestion with one possible missed cleavage, static modifications for carbamidomethyl (C), and dynamic/flexible modifications for oxidation (M). For X! Tandem we also selected parameters that allowed a quick check for protein N-terminal residue acetylation, peptide N-terminal glutamine ammonia loss, or peptide N-terminal glutamic acid water loss. Result files were submitted to the Scaffold 4 software (version 4.0.7) for validation and meta-analysis. We used the local false discovery rate scoring algorithm with standard experiment-wide protein grouping. For the evaluation of peptide and protein hits, a false discovery rate of 5% was selected for both. False positive identifications were based on reverse database analysis. We also set protein annotation preferences in Scaffold to highlight Swiss-Prot accessions among others in protein groups.

The homologous proteins were searched with the use of the blastp (version 2.2.28+) program in the UniProt human protein knowledgebase (version 2013 03) and the International Protein Index human database (version 3.87) for a comparison of the proteins identified in our study with those described by Elschenbroich *et al.* (10), Gortzak-Uzan *et al.* (3), and Drabovich and Diamandis (8). The sequences were considered homologous if the identity value was at least 90%.

Isolation of Exosomes from Ascites—Exosomes were purified via differential centrifugation as described previously (44), with some modifications. For each sample, 200 μl of ascites was diluted with 1.8 ml of PBS and centrifuged for 30 min at 10,000 $\times$ *g* in an F-45–24-11 rotor (Eppendorf, Hamburg, Germany) at 4 °C. The supernatant was carefully collected and centrifuged for 70 min at 100,000 $\times$ *g* in a Ti60 rotor (Beckman) at 4 °C to pellet exosomes. Additional exosome purification was performed via three-step sucrose gradient (48%, 40%, and 15% w/v) centrifugation in an MLS-50 rotor (Beckman). The 100,000*g* pellet was dissolved in 600 μl of 48% (w/v) sucrose. 500 ml

of 40% sucrose were overload on the first layer. The third low-density layer was formed by 4 ml of 20% sucrose. The tubes were centrifuged at 200,000 × *g* for 4 h in the MLS-50 rotor (Beckman) at 4 °C. The exosomes floated on 40% sucrose and the exosomes concentrated on the border between layers of 40% and 48% sucrose were collected, washed twice with PBS buffer, and concentrated using Agilent Technologies 30k filters.

Particle size distribution and concentration were measured on a Nanosight LM10 HS-BF instrument (Nanosight Ltd, Salisbury, UK) on the basis of nanoparticle tracking analysis. The measurements were performed using an EMCCD Andor Luca camera and a 65-mW laser at 405 nm. Samples were diluted with PBS (pH 7.4) to reach the optimal concentration for nanoparticle tracking analysis (45). Measurements were done in several repeats (5 to 12) to get at least 5000 particles in total.

RNA Isolation and RT-PCR—Total RNA was isolated using the SV Total RNA Isolation System (Promega, Madison, Wisc) with DNase treatment according to the manufacturer's protocol. cDNA was synthesized using mouse MLV reverse transcriptase (Promega). Quantitative RT-PCRs were run in triplicate on a CFX96 thermal cycler (Bio-Rad) utilizing either SYBR green or Taqman primer probe sets as noted in the supplemental "Materials and Methods" section. Real-time data were analyzed with CFX Manager software (Bio-Rad). All target RNA levels were normalized to 18S expression levels. Primer specificity was confirmed by visualizing DNA on an agarose gel following PCR.

Cell Culture—SK-OV-3 cells were grown in McCoy's 5A Modified Medium (M4892, Sigma) supplemented with 2.2 g/l sodium bicarbonate and 10% fetal bovine serum in a humidified 5% CO_2 incubator at 37 °C. For serum deprivation experiments, cells were plated in a 75T flask, washed three times with serum-free media (DMEM (D5030, Sigma) supplemented with 0.3 g/l glucose, 0.584 g/l L-glutamine, and 3.7 g/l sodium bicarbonate), and then grown in serum-free media for 24 h.

Fractionation of Culture Medium—The serum-free medium was collected and centrifuged at 2000 × *g* for 20 min to remove apoptotic bodies. Next microvesicles were pelleted via centrifugation at 16,000 × *g* for 20 min. The supernatant from this step was centrifuged at 120,000 × *g* for 70 min to pellet the exosome particles (supplemental Fig. S3). The final supernatant was concentrated to a volume of 0.3 ml using Agilent Technologies 5k filters. The microvesicle and exosome pellets were washed in PBS and resuspended in 0.3 ml of PBS.

In-solution Trypsin Digestion of Different Culture Medium Fractions—Denaturing buffer (8 M urea, 2 M thiourea, 10 mM Tris-HCl, pH 7.5) was added to the culture medium fractions (pellets and supernatant) at a ratio of 1:3, and the samples were incubated at 24 °C for 30 min. Protein disulfide bonds were reduced with 5 mM DTT at 50 °C for 30 min and then alkylated with 10 mM iodoacetamide at room temperature for 20 min in the dark. Alkylated samples were diluted by the addition of 50 mM ammonium bicarbonate solution at a ratio of 1:4; trypsin (0.01 μg per 1 μg of protein) was added, and the samples were incubated at 37 °C for 12 h. After 12 h the reaction was stopped by the addition of formic acid up to a final concentration of 5%. Finally, the tryptic peptides were desalted using Discovery DSC-18 (1-ml tubes, 50 mg) (Sigma-Aldrich, St. Louis, MO), vacuum-dried, and stored at −80 °C before LC-MS/MS analysis.

The other methods used in this study (total protein assay and immunoblot analysis) are described in the supplemental "Materials and Methods" section.

RESULTS

Determination of Ovarian Cancer Biomarkers in Ascites Samples—Ten ovarian cancer ascites and five portal alcoholic cirrhosis ascites samples were used in this study. Detailed characteristics of the biological specimens are presented in the supplemental "Materials and Methods" section.

Concentrations of the basic ovarian cancer biomarkers CA125 and HE4 that are presently used in clinical diagnostics were measured in the ascites samples via ELISA (Fig. 1*A*, supplemental "Materials and Methods"). The levels of CA125 and HE4 were increased in both types of ascites (malignant and cirrhosis) relative to the reference values (14). Moreover, ascites levels of HE4 were significantly increased in ovarian cancer patients relative to the cirrhosis group.

Metabolic Profiles of Ascitic Fluids—Our GC-MS-based metabolomic analysis of ascites derived from patients with ovarian cancer and portal alcoholic cirrhosis resulted in the detection of 129 compounds, and 89 of these compounds were identified as known metabolites. The principal component analysis score plot (Fig. 1*B*) demonstrated the separation trends between malignant and cirrhosis ascites. Forty-one compounds were considered statistically different according to the nonparametric Wilcoxon–Mann–Whitney test ($p < 0.05$) with Benjamini–Hochberg adjustment for p values (Table I). More than one-third of these compounds were identified only in the malignant ascites. 2-Hydroxyisovalerate was found to be the most depleted among the other metabolites in Table I, whereas glucose-1-phosphate was the most increased metabolite in the malignant ascites. Also, glycolate, glucose, furanose, and fructose were significantly decreased in the malignant ascites relative to the control cirrhosis samples, whereas glycero-3-phosphate, cholesterol, ceramide (d1c18:1), and MAG (18:0/0:0/0:0) were significantly elevated.

Proteome Analysis of Ascitic Fluids—We compared the proteomes of ascites from patients with ovarian cancer and from patients with portal alcoholic cirrhosis and benign neoplasms (previously published proteome dataset (10)).

The proteome of ascites, similar to the proteome of blood plasma/serum, contains a few high-abundance proteins contributing ~65% to 97% of the total protein content in a sample. The high dynamic range of protein concentrations in these biological fluids (more than 10 orders of magnitude (15)) significantly complicates their proteomic analysis. This problem can be solved by the application of various methods for preliminary fractionation of the examined material prior to its mass spectrometry analysis (3, 8–10, 16). To reduce the dynamic range of protein concentrations in biological fluids, we used one-bead one-compound CPLLs with subsequent low-percent SDS-PAGE separation of the isolated proteins. CPLL treatment of samples is known to result in 3% to 7% protein loss (16); therefore, we also fractionated the samples via low-percent SDS-PAGE without preliminary CPLL treatment. Further, the protein fractions were subjected to the reduction and alkylation of disulfide bonds with subsequent in-gel trypsin digestion and LC-MS/MS analysis (Fig. 1*C*).

In total, we identified 2096 proteins in the ovarian cancer ascites (supplemental Table S2). This value is several times

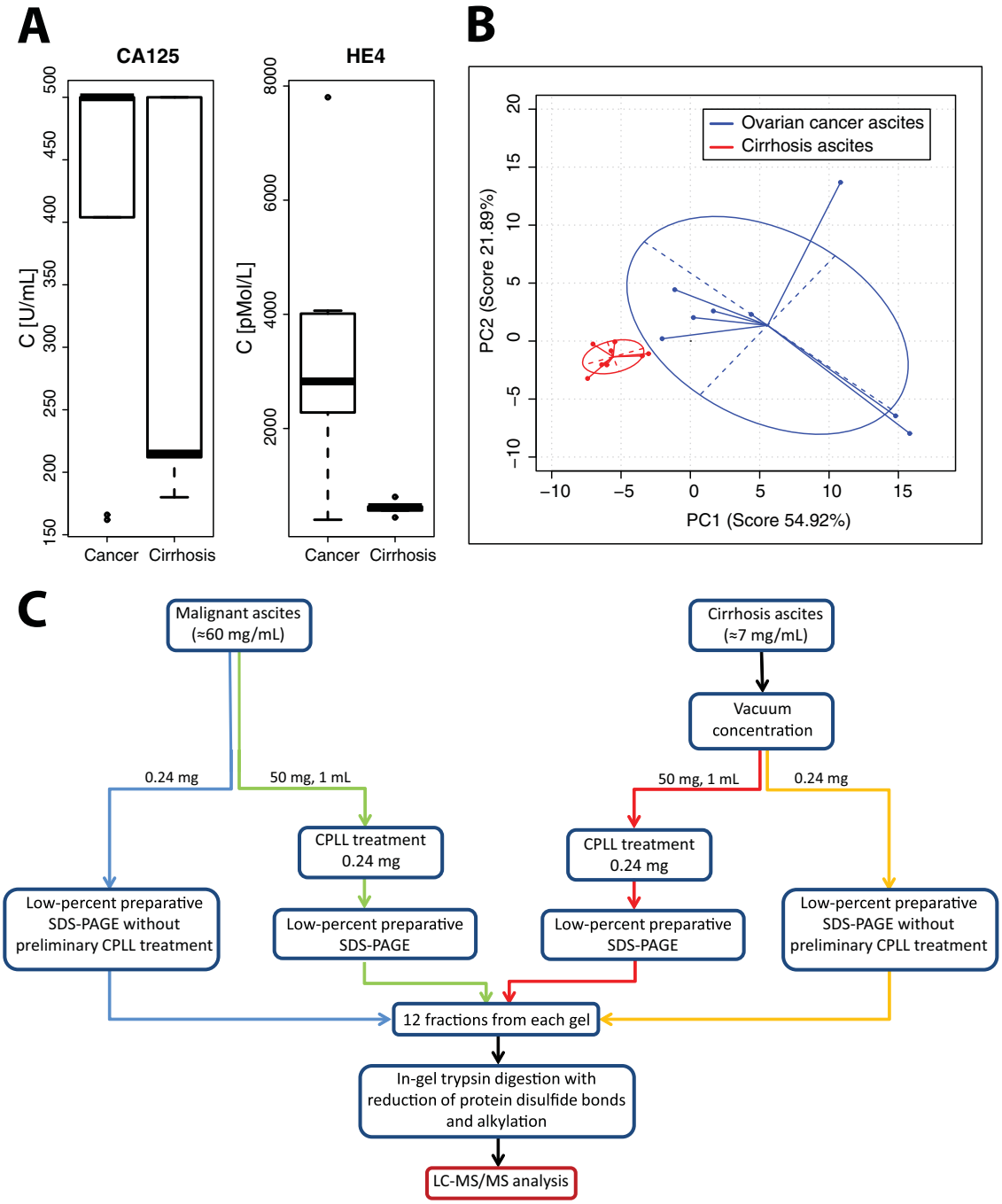

FIG. 1. **Characterization of ovarian cancer and cirrhosis ascites.** *A*, levels of ovarian cancer biomarkers CA125 (*left* panel) and HE4 (*right* panel) measured via ELISA in 10 malignant ascites (cancer) and 5 cirrhosis ascites (control) samples. *B*, the principal component analysis score plot of all identified metabolites ($n = 89$) representing significant differences in metabolites between malignant (blue) and cirrhosis (red) ascites. *C*, an integrated approach to the discovery of proteins in malignant and cirrhosis ascites.

greater than previously published data (229 (3), 445 (9), and 484 (8)). Comparison of the total list of proteins that were identified in ovarian cancer ascites in the current study with summarized data from previous studies (626 proteins (8)) gave an overlap of 77%. Our results demonstrate that the combined application of the two approaches (with and without CPLL) with subsequent low-percent SDS-PAGE fractionation of ascites proteins before their mass spectrometric analysis considerably increased the number of identified proteins. The distribution of proteins identified in malignant and cirrhosis ascites in each experiment is presented in Figs. 2*A* and 2*B*.

We compared the results of our proteomic studies with the list of potential ovarian cancer biomarkers established by Kuk

TABLE I
Differential metabolites of malignant and cirrhosis ascites derived from GC-MS analysis with the Wilcoxon–Mann–Whitney test

Metabolite name	$\log_2$ (malignant/cirrhosis ascites)	Retention time	*p* value	*p*, adjusted
Amide of linoleic acid (aC18:2)	+	24.64	7.64E-02	1.33E-01
Amide of oleic acid (aC18:1)	+	24.74	1.28E-02	3.46E-02
Amide of pentadecanoic acid (aC15:0)	+	21.86	1.28E-02	3.46E-02
Amide of stearic acid (aC18:0)	+	25.11	4.57E-03	2.02E-02
Arachidic acid (aC20:0)	+	29.84	1.28E-02	3.46E-02
Arachidonic acid (ac20:4)	+	28.89	4.57E-03	2.02E-02
Behenic acid (ac22:0)	+	32.35	7.64E-02	1.33E-01
Capric acid (aC10:0)	+	13.74	1.46E-03	1.36E-02
Ceramide (d1c18:1)	+	43.68	4.57E-03	2.02E-02
Cholesta-4,6-dien-3-ol	+	35.23	1.46E-03	1.36E-02
Cholesteryl acetate	+	35.09	4.53E-03	2.02E-02
Docosahexaenoic acid (aC22:6)	+	31.39	4.57E-03	2.02E-02
Eicosadienoic acid (aC20:2)	+	29.45	1.71E-01	2.22E-01
Eicosenoic acid (aC20:1)	+	29.51	1.28E-02	3.46E-02
Glycero-3-phosphate	+	19.97	1.36E-02	3.62E-02
Lauric acid (ac12:0)	+	17.53	8.26E-04	1.34E-02
Lignoceric acid (ac24:0)	+	34.71	7.64E-02	1.33E-01
Lysophosphatidic acid 16:0	+	37.32	1.28E-02	3.46E-02
Monoacylglycerol (18:1/0:0/0:0)	+	33.95	1.28E-02	3.46E-02
Methyl phosphate (2TMS)	+	8.12	4.10E-04	8.88E-03
Myristic acid (aC14:0)	+	21.01	2.19E-02	5.48E-02
nOH14:0	+	19.55	1.28E-02	3.46E-02
Palmitoleic acid (aC16:1)	+	23.87	1.27E-02	3.46E-02
Glucose-1-phosphate	4.6	27.24	1.22E-02	3.46E-02
Stearic acid (aC18:0)	2.7	27.14	1.35E-03	1.36E-02
Cholesterol	2.6	38.46	1.55E-04	6.73E-03
Linoleic acid (aC18:2)	2.5	26.69	9.31E-04	1.34E-02
Palmitic acid (aC16:0)	1.6	24.21	2.95E-03	2.02E-02
Oleic acid (aC18:1 1)	1.4	26.85	1.25E-01	1.98E-01
Vaccenic acid (aC18:1 2)	1.2	26.76	2.95E-03	2.02E-02
Glycolate (2TMS)	−1.6	6.12	1.55E-04	6.73E-03
2-Hydroxybutanoate (2TMS)	−1.8	7.09	3.11E-04	8.88E-03
Furanose	−3.1	21.38	1.48E-02	3.84E-02
Glucose	−3.4	22.26	1.09E-03	1.36E-02
Fructose	−4.9	21.45	6.22E-04	1.15E-02
Galacturonic acid	−5.0	22.12	1.89E-03	1.64E-02
2-Hydroxyisovalerate (2TMS)	−5.1	7.83	1.55E-04	6.73E-03
2,4-Dihydroxybutanoate (3TMS)	−	13.07	1.28E-02	3.46E-02
Pyranose 1853	−	20.99	1.28E-02	3.46E-02
Sorbitol	−	23.05	4.10E-04	8.88E-03
Xylitol	−	19.07	1.28E-02	3.46E-02

Notes: +, metabolites that were not identified in cirrhosis ascites; −, metabolites that were not identified in malignant ascites; TMS, trimethylsilyl (protecting group).

The positive and negative values of $\log_2$ (malignant/cirrhosis ascites) indicate a relatively higher or lower concentration, respectively, in the malignant ascites in comparison with the cirrhosis ascites.

et al. (9) on the basis of literature data and found 29 of 39 possible protein biomarkers of ovarian cancer (supplemental Table S3). However, 23 of these 29 proteins were also identified in the cirrhosis samples.

Comparison of the protein lists of malignant, benign (previously published proteome dataset (10)), and cirrhosis ascites allowed us to reveal the proteins specific to malignant ascites and remove those proteins that were part of a systemic response to ascites formation (supplemental Table S3). In general, this strategy allowed the identification of 424 proteins specific to malignant ascites (Fig. 2*C*). To confirm the LC-MS/MS identification results, we examined several proteins important for cancer cells via immunoblot analysis: TGM2 (extracellular matrix protein (17)), Hsp90 (intracellular and exosomal protein (18)), U2AF1, U2AF2, HNRNPA2B1, and HNRHPU (intracellular spliceosomal proteins (19)) (Fig. 3*C*). According to the immunoblot results, the amount of Hsp90 was significantly greater in cancer samples, which coincided with our LC-MS/MS data, in which the number of spectra identified as peptides of Hsp90 was 14.5 times higher in malignant ascites than in cirrhosis ascites. TGM2, U2AF1, U2AF2, and HNRHPU were exclusively detected in cancer

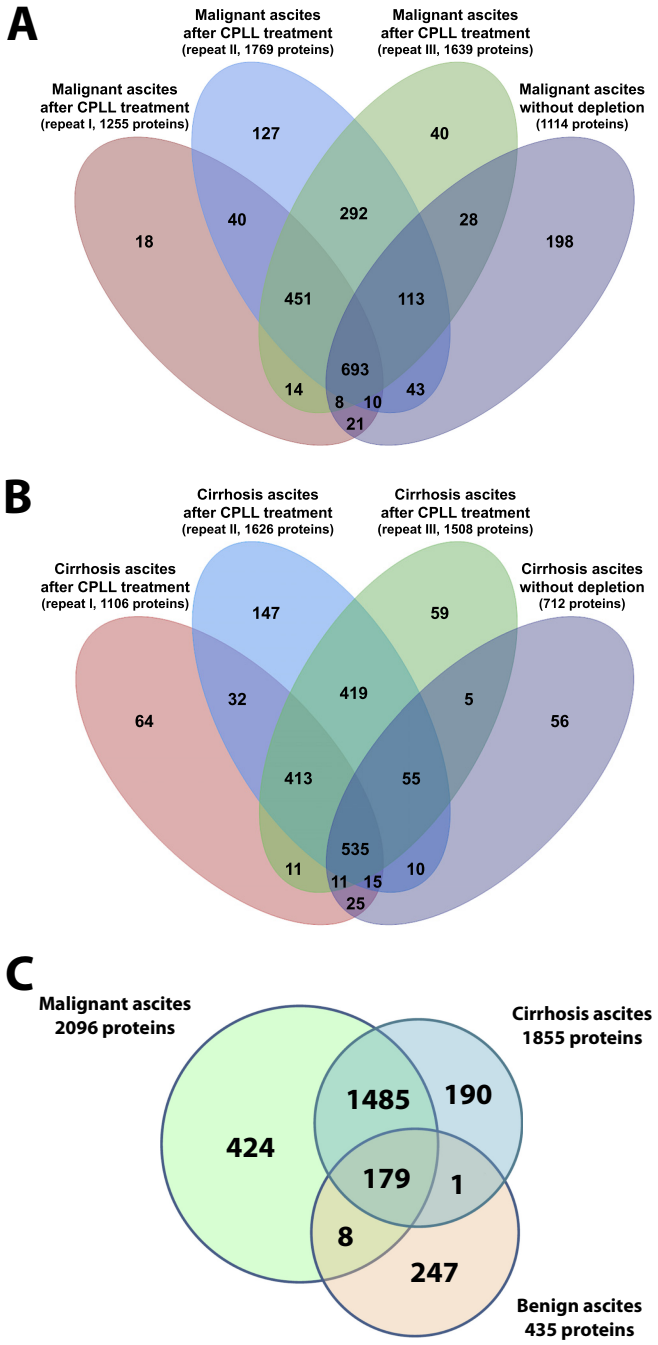

FIG. 2. **Distribution of proteins identified in malignant (*A*) and cirrhosis ascites (*B*) in individual experiments (with and without CPLL treatment).** *C*, comparative analysis of the proteomes of malignant (green circle), cirrhosis (blue circle), and benign ascites (pink circle).

samples in both immunoblot and LC-MS/MS analyses. Proteome data for HNRNPA2B1 were not verified using immunoblotting. Summing up, we confirmed five of the six examined proteins.

Analysis of the list specific to malignant ascites with the use of the UniProtKB, NCBI, and ExoCarta databases showed that the majority of these proteins could be secreted from the cells: 34% of the proteins are extracellular, and 40% were found within exosomes (Fig. 4*A*).

The elevated number of exosomal proteins in the malignant ascites could be associated with the increased production of exosomes by cancer cells. We checked this using the method of nanoparticle tracking analysis for the calculation of exosomes in the malignant and cirrhosis samples. As follows from Figs. 4*B* and 4*C*, the number of vesicles that were isolated from malignant ascites was significantly greater than that from the cirrhosis samples. This conclusion is in good agreement with our proteomic data.

Functional Analysis of the Identified Proteins—We analyzed the lists of identified proteins from the malignant and cirrhosis ascites using the STRING online service with KEGG, GO Cell Component, GO Biological Process, and NCI databases and reliably revealed more than 100 clusters of interacting proteins ($p < 0.01$). According to the analysis of these databases, the cluster of spliceosomal proteins (proteins participating in pre-mRNA splicing) was high on the list (supplemental Table S4). In particular, the analysis with the use of the KEGG database demonstrated that the differences in the cluster of spliceosome proteins were the most pronounced among the compared samples (supplemental Table S4 and Fig. 3*A*). Similar data were acquired using the GO Cell Component database (supplemental Table S4 and Fig. 3*B*). The most pronounced differences (7-fold and less) in the protein occurrence were found for the components associated with RNA splicing: U12-type spliceosomal complex, U4 snRNP, pICln-Sm protein complex, methylosome, U1 snRNP, SMN-Sm protein complex, catalytic step 2 spliceosome, and spliceosomal complex. Relationships between the aforementioned terms are illustrated in an ontology graph that was plotted with the use of the OBO-Edit software (supplemental Fig. S1). Similar data were obtained using the NCI and GO Biological Process databases (supplemental Table S4).

These data are of special interest because the splicing process in cancer cells is known to be considerably different from that in normal cells (20–22), and several spliceosomal proteins have been shown to be promising targets for chemotherapy (23, 24).

Detection of Spliceosomal RNAs in Ascitic Fluids—Spliceosomal proteins fulfill their functions in complex with a special type of small nuclear uridine-rich RNA (snRNA). They form macromolecular ribonucleoprotein complexes (RNPs) called spliceosomes. At present, two types of spliceosomes are known: major (U2-type) and minor (U12-type). U1, U2, U4, U5, and U6 snRNAs are parts of the major spliceosome, and U11, U12, U4atac, U5, and U6atac snRNAs are present in the minor spliceosome. The minor spliceosome content of a cell is 100 times less than the major one.

We decided to check for the presence of splicing RNA in the examined ascites samples, because the greatest differences in protein occurrence revealed by proteome analysis

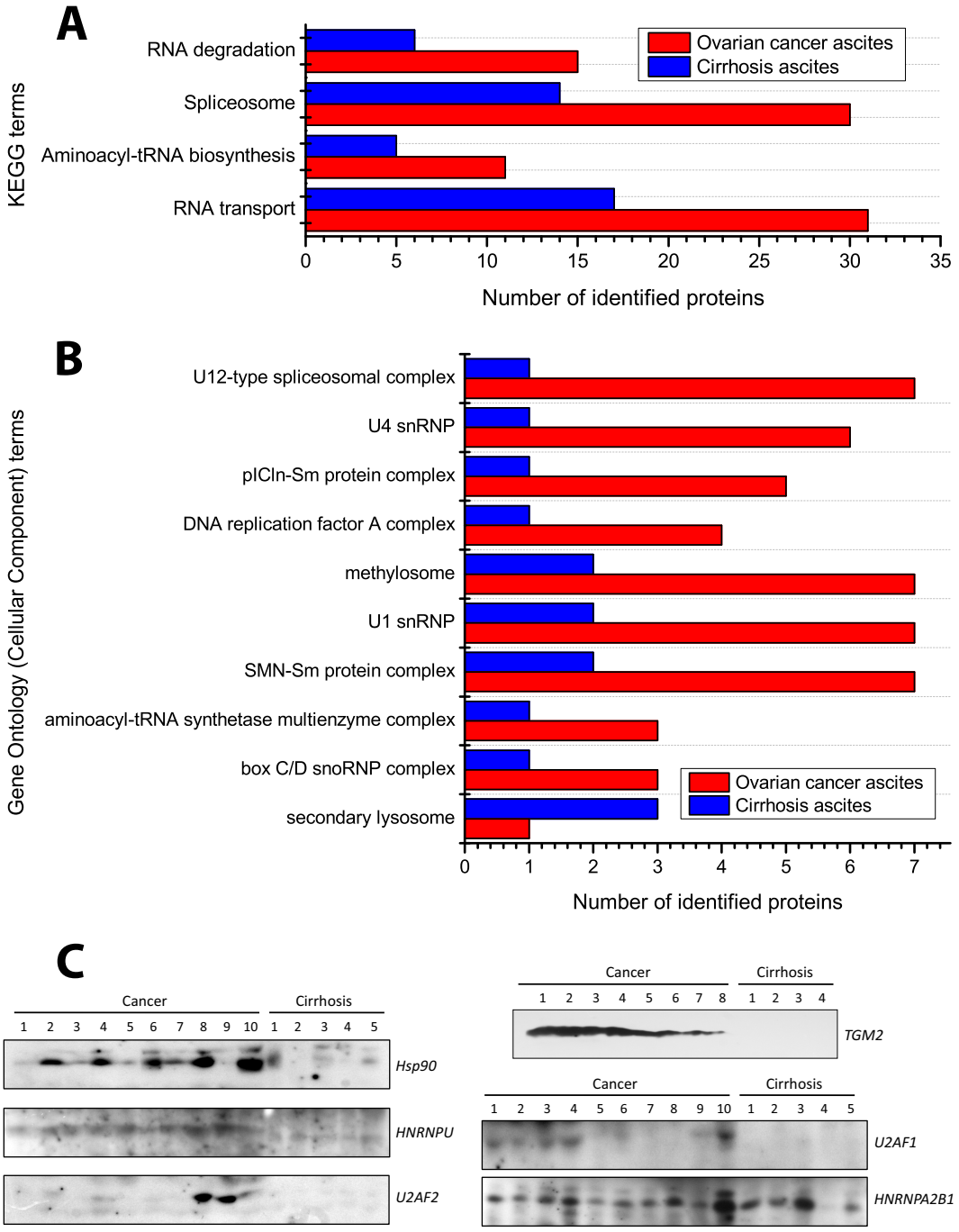

FIG. 3. **Functional analysis of ascites proteome data by the STRING online service.** *A*, statistically significant ($p < 0.01$) clusters of proteins that occurred differentially in samples of the compared groups detected with the use of the KEGG database. *B*, statistically significant clusters (the first 10 terms) of proteins that occurred differentially in samples of the compared groups detected with the use of the GO Cell Component database. *C*, amount of HSP90, HNRNPU, U2AF2, TGM2, U2AF1, and HNRNPA2/B1 in malignant and cirrhosis ascites determined via Western blotting.

are related to splicing-associated proteins. The results of the experiment regarding the determination of the relative content of the major spliceosome snRNAs in control and malignant ascites are presented in Fig. 5*A*.

As follows from the data, the greatest difference in the content of snRNAs in the tested samples was observed for the U6 snRNA (Fig. 5*A*). However, comparison of U6 snRNA content in all examined samples (Fig. 5*B*, light bars) demonstrated significant differences among the malignant samples and approximately the same levels in all control samples. The amount of U6 snRNA was considerably increased in seven out of nine malignant ascites relative to the control, but in two

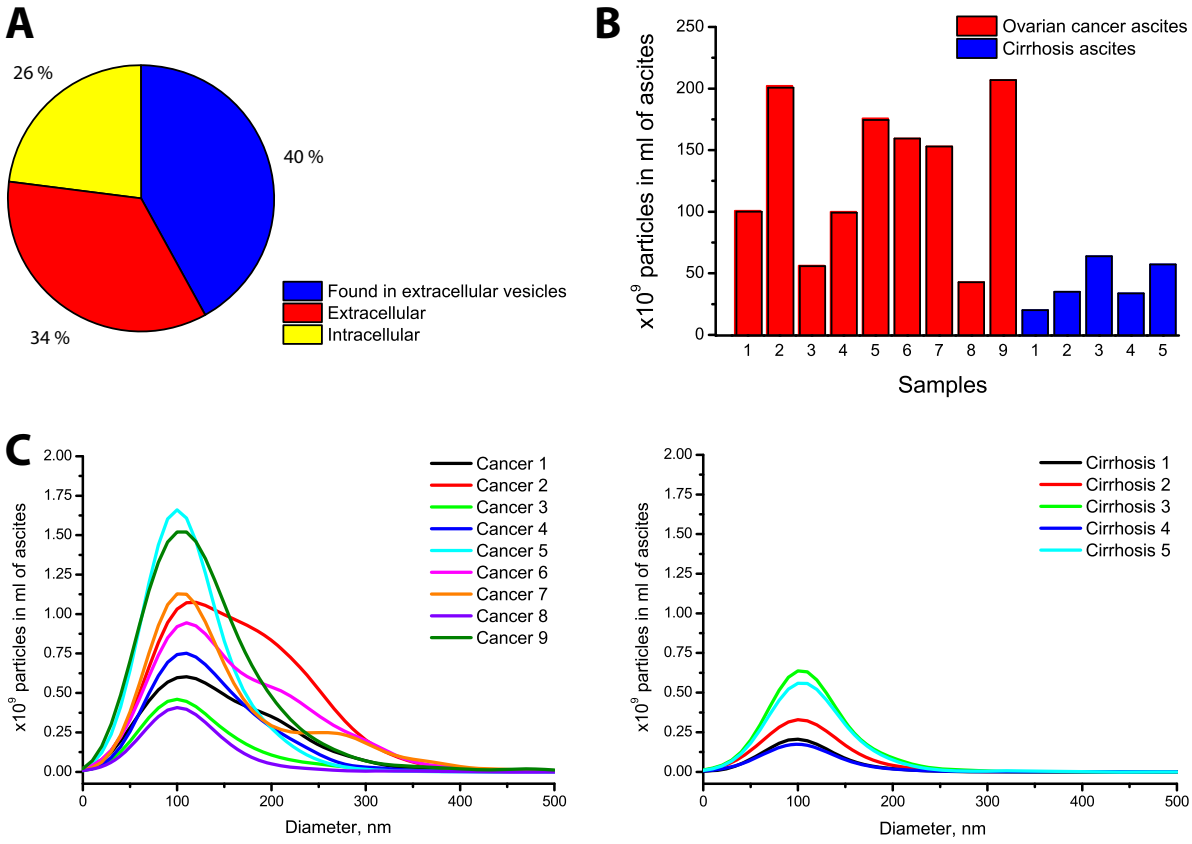

FIG. 4. **Comparison of extracellular vesicles present in malignant and cirrhosis ascites.** *A*, localization of the proteins unique to the malignant ascites: extracellular (red), intracellular (yellow), and found in extracellular vesicles (microvesicles and exosomes) (blue). *B*, amount of exosomes isolated from malignant (red) and cirrhosis (blue) ascites. *C*, size distribution of exosomes that were isolated from malignant (*left* panel) and cirrhosis (*right* panel) ascites.

malignant samples it was lower than that in the control samples. Then we studied components of the minor spliceosome. Analysis of snRNAs of the U12 spliceosome demonstrated that all types of minor spliceosome snRNAs (U11, U12, U4atac, and U6atac) were present in the malignant ascites, whereas only U11 snRNA was detected in the control ascites (data not shown). Fig. 5*B* (dark bars) illustrates the comparison of the amount of U12 snRNA in all the examined samples. As follows from Fig. 5*B*, this RNA was present in all of the malignant ascites but was not detected in any of the control samples. These results correlate well with our proteomic data (Fig. 3*B*), in which the major difference between malignant and cirrhosis ascites was observed for the proteins of the minor spliceosome.

Searching for the Possible Mechanisms Underlying the Appearance of Splicing RNPs in Malignant Ascites—To the best of our knowledge, this is the first report demonstrating the presence of spliceosomal RNA in the extracellular medium. Evidently, RNPs could be released into the extracellular medium as a result of the apoptosis/necrosis-induced leakage of intracellular content, or they could be specifically exported from cancer cells. To explore both possibilities, we compared the relative contents of U12 snRNA in cells of ovarian adenocarcinoma (SK-OV-3) and in ovarian cancer ascites. For this purpose, the amount of U12 snRNA was normalized to that of the 18S ribosomal RNA. This normalization method was chosen because 18S rRNA and U12 snRNA must be released together into the ascitic fluid as a result of lysis of cancer cells. However, the U12 snRNA/18S rRNA ratio in the ascites would be significantly higher than the same ratio inside the cell if U12 snRNA were specifically exported from the cell. As follows from Fig. 5*C*, the relative content of U12 snRNA outside the cell was more than 10,000 times greater than that inside the cell. It is important to note that this result was not associated with the differences in stability of the examined RNA types in the extracellular medium (supplemental Fig. S2). The above-mentioned results provide evidence of the active export of U12 snRNA to the extracellular medium, rather than apoptosis or necrosis leakage to the ascitic fluid.

RNA could be exported from the cells in complexes with special carrier proteins or by exosomes and microvesicles (25–27). We analyzed the fractions obtained after differential centrifugation of ascites to determine whether U12 snRNA was localized within the vesicles. After centrifugation at both 16,000 × *g* and 120,000 × *g*, the most U12 snRNA was detected in the supernatant (Fig. 5*D*). These results suggest

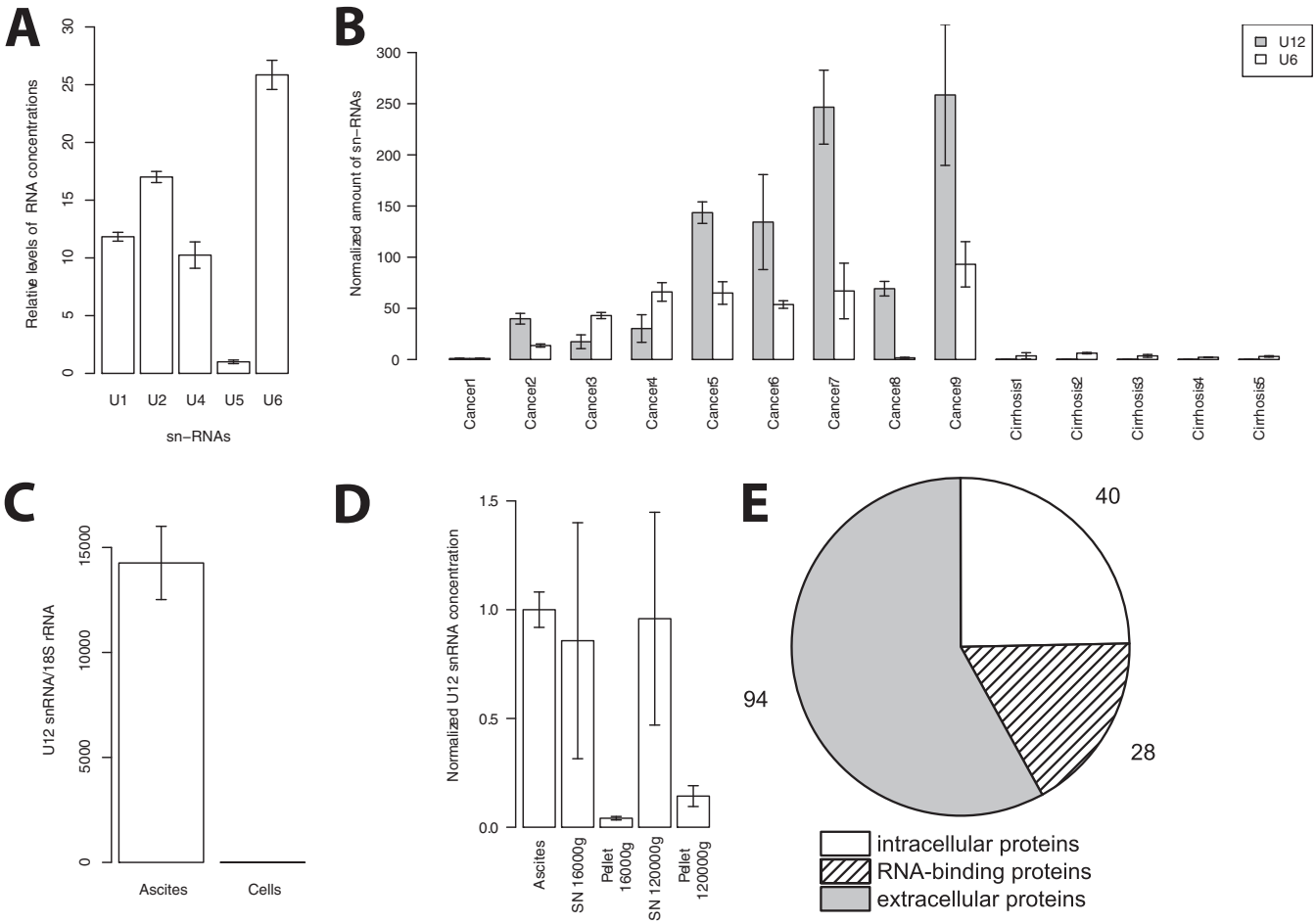

FIG. 5. **Analysis of splicing RNAs in ascites.** *A*, relative increase in the quantity of major spliceosome snRNAs in malignant ascites in comparison with the control sample. *B*, the normalized amount of U6 RNA (light bars) and U12 RNA (dark bars) in malignant and cirrhosis ascites. *C*, relative content of the U12 snRNA in ovarian adenocarcinoma cells and in malignant ascites. *D*, normalized amount of U12 RNA in the fractions obtained after differential centrifugation. *E*, analysis of vesicle-free proteins secreted by SK-OV-3 cells: extracellular (gray), 58% localization; intracellular (white), 42% localization. The most abundant proteins from the non-vesicle fraction were related to the RNA-binding protein cluster (41.2%).

that U12 snRNA is present in ascites within a nonsedimentary protein complex.

To confirm this result we examined the proteins exported from ovarian cancer cells *in vitro*. SK-OV-3 cells were grown for 24 h in serum-free medium, and then vesicle-associated and free proteins were separated via differential centrifugation and profiled via mass spectrometry (supplemental Fig. S3).

Functional analysis of proteome data demonstrated that the most abundant proteins from the non-vesicle fraction were related to the RNA-binding protein cluster (41.2%) according to the KEGG database (Fig. 5*E*). This fraction was statistically significantly enriched ($p < 0.05$) with spliceosomal proteins. A total of seven spliceosomal proteins were identified: NONO, ALY, YBX1 (specific component of U12 spliceosome (28)), HNRNPA1, HNRNPA2B1, HNRPA3, and RBMX. It is important to note that we did not identify any spliceosomal proteins in the vesicle-associated fraction, and there was not any enrichment with RNA-binding protein (supplemental Table S6).

DISCUSSION

Ascites Metabolome—The GC-MS-based metabolomics study demonstrated that the levels of 41 metabolites of malignant and cirrhosis ascites differed considerably. The most important differences were found for fatty acids, cholesterol, ceramide, glycerol-3-phosphate, glucose, and glucose-3-phosphate (Table I).

The decreased glucose level in the malignant ascites, relative to the cirrhosis ascites, could be associated with the Warburg effect (29). This effect consists of a shift of the mitochondrial functions from energy generation to the production of intermediates for biosynthesis. This hypothesis is indirectly confirmed by the fact that we identified TGM2 in the examined proteomes exceptionally in cancer samples (sup-

plemental Table S2, Fig. 3*C*). Aberrant expression of TGM2 has previously been shown to be an important regulator of the Warburg effect in mammary epithelial cells (17).

Derivatives of fatty acids are another metabolic class by which the malignant ascites was considerably distinguished from the control. It is known that oncogenic signaling contributes both directly and indirectly to the up-regulation of pathways of fatty acid synthesis (30, 31). Lipids, their fatty acids, and amides of the fatty acids not only provide cells with energy, but are important signaling molecules and modulators for the transduction of intracellular signals, interfere with oxidative metabolism, and can affect gene expression as ligands for specific nuclear receptors. Derivatives of fatty acids such as ceramides can also be secondary messengers (32). One such molecule, ceramide (18:1), was identified only in the malignant ascites in our study.

Lysophosphatidic acid identified in our metabolomics study was present only in the malignant ascites; it is an idiopathic microenvironmental factor of ovarian cancer. Its level is known to be increased in the blood and ascites of ovarian cancer patients. Multiple pieces of evidence point to the involvement of lysophosphatidic acid in the signaling cascades that facilitate the initiation, development, and dissemination of ovarian cancer. Moreover, lysophosphatidic acid induces the formation of inflammatory cytokines, which favor the survival of malignant cells and predetermine their more aggressive behavior (33–35).

Thus, increased levels of biosynthesis of fatty acids and cholesterol are characteristic of cancer cells. The phenomenon can result in increased amounts of lipids with various signaling functions, which may contribute to cancer development.

Ascitic Proteome—The comprehensive approach to sample preparation (with and without CPLL treatment with subsequent low-percent SDS-PAGE fractionation) resulted in the identification of 2096 proteins in malignant ascites. Some of these proteins perform their functions inside the cell. In previously published works, intracellular proteins (including those proteins that were present both inside a cell and in extracellular vesicles) were discarded from searches of potential ovarian cancer biomarkers (3, 8–10) in ascites. We decided to avoid such a strategy and studied all the identified proteins.

Several mechanisms of penetration of non-secretory proteins into the extracellular space are known. First, they may be present in apoptotic bodies that appear as a result of programmed cell death, or they can be released into the extracellular space during necrosis. Second, a considerable number of proteins may be present in extracellular vesicles (such as microvesicles and exosomes). Taylor and Gercel-Taylor (26) have demonstrated that ovarian cancer cells produce increased numbers of exosomes relative to control and benign samples. Third, it has been repeatedly reported that large RNA-containing protein complexes can be exported from cancer cells via an unknown mechanism that is not associated with vesicles (25, 27). All the above-mentioned data convincingly suggest that the intracellular proteins should not be excluded from consideration in the analysis of ascites and other biological fluids.

As follows from Fig. 4*A*, intracellular proteins that can be exported from cells within exosomes constitute a considerable number of the proteins identified by us as unique to malignant ascites. This fact can be explained by the increased content of exosomes in the malignant ascites. These exosomes can transport proteins important for signal transduction both between the cancer cells and from these cells to normal adjacent tissues, for example, for the stimulation of angiogenesis (36).

Functional analysis of all the proteins that were identified in the malignant and cirrhosis ascites demonstrated that the greatest difference in the quantity of the proteins between the compared samples was observed in the cluster of spliceosomal proteins. We attributed 65 proteins to this cluster on the basis of the proteomic data (supplemental Table S5). The presence of these proteins in the malignant samples could reflect an important special feature of cancer cells that is associated with multifold disorders in processes of RNA splicing. It is known that significant changes in the expression of various splicing factors and dramatic post-translational modifications of these proteins occur during cancer transformation, and a lot of mutations that considerably affect protein activities and functions also take place (20–22). We identified most of the spliceosomal proteins that previously have been shown to be hyperexpressed in ovarian cancer cells (37) (supplemental Table S5). This result was of special interest because Quidville *et al.* demonstrated that some spliceosomal components hyperexpressed in cancer cells participate in the regulation of the PI3K/Akt/mTOR pathway, which is often disturbed in ovarian cancer (38). Thus, spliceosome components are attractive targets for anticancer therapy.

Analysis of Splicing RNAs in Ascites—Analysis of RNA in various biological fluids has demonstrated that a large number of short non-coding RNAs are present in the extracellular medium (27, 39). It was proposed earlier that these RNAs are protected from degradation by encapsulation in extracellular secreted vesicles (microvesicles and exosomes). However, the latest data provide evidence that this is not the only way that RNA exists in the extracellular space. Several papers have shown that most of the extracellular non-vesicle-associated miRNAs are present in blood plasma in complexes with the Ago2 protein (the key effector protein of miRNA-mediated silencing) (40, 41). Some miRNAs are protected from degradation in the blood flow owing to association with high-density lipoproteins (HDLs) (42). Finally, Wang *et al.* identified 12 different RNA-binding proteins that can form complexes with miRNA and export it from cancer cells (27). It is important to note that 11 of these 12 proteins were identified in our study (Table II).

miRNA is not the only type of RNA found in the extracellular medium. There is evidence that other RNA types, such as rRNA, tRNA, and sno- and snRNA, are present in the extra-

TABLE II
Identification of RNA-binding proteins capable of miRNA export (27) in malignant and cirrhosis ascites

Gene symbol	Number of peptides observed in Ref. 27	Gene name	Number of peptides observed in our data	
			Ovarian cancer ascites	Cirrhosis ascites
HNRNPA2B1	2	Heterogeneous nuclear ribonucleoprotein a2/b1	1	–
HNRPAB	3	Heterogeneous nuclear ribonucleoprotein a/b	–	–
ILF2	2	Interleukin enhancer binding factor 2, 45 kda	18	6
NCL	7	Nucleolin	16	–
NPM1	4	Nucleophosmin (nucleolar phosphoprotein b23, numatrin)	3	–
RPL10A	2	Ribosomal protein 10a	2	–
RPL5	2	Ribosomal protein 5	7	1
RPLP1	6	Ribosomal protein, large, p1	3	1
RPS12	2	Ribosomal protein s12	6	5
RPS19	2	Ribosomal protein s19	2	1
SNRPG	2	Small nuclear ribonucleoprotein polypeptide G	2	–
TROVE2	2	Trove domain family, member 2	3	3

cellular medium. However, most of the studies have paid attention to miRNA as the most abundant class of extracellular RNA.

We determined the content of splicing snRNAs in malignant and cirrhosis ascites. We found that U12 snRNA (a component of the U12 spliceosome) was present in all the malignant ascites and was not detected in the control samples. We demonstrated that apoptosis/necrosis was not responsible for the presence of splicing RNA in the extracellular medium and proposed that the splicing RNA was transported to the extracellular space from the cancer cells via a specific export mechanism. We determined, using differential centrifugation, that the major part of U12 snRNA was not encapsulated in the extracellular vesicles. This result was confirmed *in vitro* using ovarian cancer cell line SK-OV-3. Possibly, the splicing U12 snRNA was transported to the extracellular medium in complex with splicing proteins, similar to the export of miRNA in complexes with Ago2, HDL, or NPM1 from cells. This hypothesis is in good agreement with the recently published data on the analysis of autoantibodies, which are present in the blood of breast cancer patients (43). Ladd *et al.* convincingly demonstrated that most autoantibodies in the blood of cancer patients and tumor-bearing mice are produced against spliceosomal proteins. The data corroborate the hypothesis of active export of these proteins from cancer cells, and they confirm our conclusion that their export is not associated with encapsulation in extracellular vesicles.

Summing up, this study extended our knowledge of the protein and metabolomic composition of ovarian cancer ascites and revealed specific features that are associated with the function of the ascites as a medium of interaction between the cancer cells and their environment. We found a wide variety of molecule types that participate in this process. Among them, low-molecular metabolites, including lysophosphatidic acid, cholesterol, different fatty acids, and their amides, were identified. These compounds can act as important signaling molecules themselves and as precursors for different hormones and growth factors. We also found an increased amount of exosomes, which are important cell-to-cell transmitters of biomolecules. Moreover, we identified a number of RNA-binding proteins responsible for the extracellular transport of miRNA. In addition, we found various components of spliceosomes (65 splicing proteins and all types of splicing RNAs) in the extracellular medium. In our view, these RNPs could also participate in cell–cell communication. Similarly to the export complexes of miRNA, we assume that spliceosomes also could act as transport carriers for RNA molecules between various cells. Our results raise significant questions about the role of spliceosomal complexes in cell–cell communication. Currently we have no direct evidence that the above-mentioned RNPs could affect neighboring cancer or normal cells; however, we suppose they could promote cancer cell survival or metastasis by affecting cancer-specific splicing changes via a yet unknown mechanism. Studies to test this hypothesis are ongoing in our group. In addition, we plan to verify whether cancer-specific U12 snRNA could be used for PCR diagnosis of ovarian cancer. In the current study, we tested only ascites samples from patients who had received several courses of chemotherapy prior to ascites collection; thus it should be further confirmed whether U12 snRNA could be detected at the early stages of the disease or appears only in recurrent tumors. In addition, it would be extremely interesting to further study the proteome of ovarian cancer ascites and compare proteomic results with the disease outcome to find possible prognostic markers that would help predict patient survival and the effectiveness of different chemotherapy methods.

The mass spectrometry proteomics data have been deposited to the ProteomeXchange Consortium via the PRIDE partner repository with the dataset identifier PXD001402 (DOI 10.6019/PXD001402) and PXD001403 (DOI 10.6019/PXD001403).

Acknowledgments—We thank Dr. Nikolaj Pestov for helpful comments on the manuscript and Dmitry Ischenko for help with manu-

script preparation. We are also grateful to the Evrogen team for their outstanding technical assistance.

* This work was financially supported by the Russian Ministry of Industry and Trade (Contract No. 074/13-FMP-31.12ok, lot "3.2-Biomarker-2014," to V. Govorun), by the Russian Foundation for Basic Research (Grant Nos. 12-04-31227, to M. Pavlyukov, and 14-04-01844, to M. Shakhparonov), and by an MCB RAS grant (to M. Shakhparonov), and partially supported by Ministry of Education and Science of the Russian Federation (grant No. 14.607.21.0068 to V. Govorun).

[S] This article contains supplemental material.

§ To whom correspondence should be addressed: Victoria Shender, Shemyakin-Ovchinnikov Institute of Bioorganic Chemistry, Miklukho-Maklaya str. 16/10, Moscow 117997, Russian Federation, E-mail: victoria.shender@gmail.com.

¶ These authors contributed to this work equally.

REFERENCES

1. Kozak, K. R., Su, F., Whitelegge, J. P., Faull, K., Reddy, S., and Farias-Eisner, R. (2005) Characterization of serum biomarkers for detection of early stage ovarian cancer. *Proteomics* **5,** 4589–4596
2. Kipps, E., Tan, D. S., and Kaye, S. B. (2013) Meeting the challenge of ascites in ovarian cancer: new avenues for therapy and research. *Nat. Rev. Cancer* **13,** 273–282
3. Gortzak-Uzan, L., Ignatchenko, A., Evangelou, A. I., Agochiya, M., Brown, K. A., St Onge, P., Kireeva, I., Schmitt-Ulms, G., Brown, T. J., Murphy, J., Rosen, B., Shaw, P., Jurisica, I., and Kislinger, T. (2008) A proteome resource of ovarian cancer ascites: integrated proteomic and bioinformatic analyses to identify putative biomarkers. *J. Proteome Res.* **7,** 339–351
4. Dunn, W. B., Broadhurst, D., Begley, P., Zelena, E., Francis-McIntyre, S., Anderson, N., Brown, M., Knowles, J. D., Halsall, A., Haselden, J. N., Nicholls, A. W., Wilson, I. D., Kell, D. B., and Goodacre, R. (2011) Procedures for large-scale metabolic profiling of serum and plasma using gas chromatography and liquid chromatography coupled to mass spectrometry. *Nat. Protoc.* **6,** 1060–1083
5. Karimi, P., Shahrokni, A., and Nezami Ranjbar, M. R. (2014) Implementation of proteomics for cancer research: past, present, and future. *Asian Pacific J. Cancer Prev.* **15,** 2433–2438
6. O'Connell, T. M. (2012) Recent advances in metabolomics in oncology. *Bioanalysis* **4,** 431–451
7. Vermeersch, K. A., and Styczynski, M. P. (2013) Applications of metabolomics in cancer research. *J. Carcinogenesis* **12,** 9
8. Drabovich, A. P., and Diamandis, E. P. (2010) Combinatorial peptide libraries facilitate development of multiple reaction monitoring assays for low-abundance proteins. *J. Proteome Res.* **9,** 1236–1245
9. Kuk, C., Kulasingam, V., Gunawardana, C. G., Smith, C. R., Batruch, I., and Diamandis, E. P. (2009) Mining the ovarian cancer ascites proteome for potential ovarian cancer biomarkers. *Mol. Cell. Proteomics* **8,** 661–669
10. Elschenbroich, S., Ignatchenko, V., Clarke, B., Kalloger, S. E., Boutros, P. C., Gramolini, A. O., Shaw, P., Jurisica, I., and Kislinger, T. (2011) In-depth proteomics of ovarian cancer ascites: combining shotgun proteomics and selected reaction monitoring mass spectrometry. *J. Proteome Res.* **10,** 2286–2299
11. Zhou, M., Guan, W., Walker, L. D., Mezencev, R., Benigno, B. B., Gray, A., Fernandez, F. M., and McDonald, J. F. (2010) Rapid mass spectrometric metabolic profiling of blood sera detects ovarian cancer with high accuracy. *Cancer Epidemiol. Biomarkers Prev.* **19,** 2262–2271
12. Odunsi, K., Wollman, R. M., Ambrosone, C. B., Hutson, A., McCann, S. E., Tammela, J., Geisler, J. P., Miller, G., Sellers, T., Cliby, W., Qian, F., Keitz, B., Intengan, M., Lele, S., and Alderfer, J. L. (2005) Detection of epithelial ovarian cancer using 1H-NMR-based metabonomics. *Int. J. Cancer* **113,** 782–788
13. Zhang, T., Wu, X., Ke, C., Yin, M., Li, Z., Fan, L., Zhang, W., Zhang, H., Zhao, F., Zhou, X., Lou, G., and Li, K. (2013) Identification of potential biomarkers for ovarian cancer by urinary metabolomic profiling. *J. Proteome Res.* **12,** 505–512
14. Ghasemi, N., Ghobadzadeh, S., Zahraei, M., Mohammadpour, H., Bahrami, S., Ganje, M. B., and Rajabi, S. (2014) HE4 combined with CA125: favorable screening tool for ovarian cancer. *Med. Oncol.* **31,** 808
15. Anderson, N. L., Polanski, M., Pieper, R., Gatlin, T., Tirumalai, R. S., Conrads, T. P., Veenstra, T. D., Adkins, J. N., Pounds, J. G., Fagan, R., and Lobley, A. (2004) The human plasma proteome: a nonredundant list developed by combination of four separate sources. *Mol. Cell. Proteomics* **3,** 311–326
16. Boschetti, E., Lomas, L., Citterio, A., and Righetti, P. G. (2007) Romancing the "hidden proteome." *J. Chromatogr. A* **1153,** 277–290
17. Kumar, S., Donti, T. R., Agnihotri, N., and Mehta, K. (2013) Transglutaminase 2 reprogramming of glucose metabolism in mammary epithelial cells via activation of inflammatory signaling pathways. *Int. J. Cancer* **134,** 2798–2807
18. McCready, J., Sims, J. D., Chan, D., and Jay, D. G. (2010) Secretion of extracellular hsp90alpha via exosomes increases cancer cell motility: a role for plasminogen activation. *BMC Cancer* **10,** 294
19. Valadkhan, S., and Jaladat, Y. (2010) The spliceosomal proteome: at the heart of the largest cellular ribonucleoprotein machine. *Proteomics* **10,** 4128–4141
20. Chen, M., and Manley, J. L. (2009) Mechanisms of alternative splicing regulation: insights from molecular and genomics approaches. *Nat. Rev. Mol. Cell Biol.* **10,** 741–754
21. Maciejewski, J. P., and Padgett, R. A. (2012) Defects in spliceosomal machinery: a new pathway of leukaemogenesis. *Br. J. Haematol.* **158,** 165–173
22. Zhou, Z., and Fu, X. D. (2013) Regulation of splicing by SR proteins and SR protein-specific kinases. *Chromosoma* **122,** 191–207
23. Laetsch, T. W., Liu, X., Vu, A., Sliozberg, M., Vido, M., Elci, O. U., Goldsmith, K. C., and Hogarty, M. D. (2014) Multiple components of the spliceosome regulate Mcl1 activity in neuroblastoma. *Cell Death Dis.* **5,** e1072
24. Bonnal, S., Vigevani, L., and Valcarcel, J. (2012) The spliceosome as a target of novel antitumour drugs. *Nat. Rev. Drug Discov.* **11,** 847–859
25. Hoy, A. M., and Buck, A. H. (2012) Extracellular small RNAs: what, where, why? *Biochem. Soc. Trans.* **40,** 886–890
26. Taylor, D. D., and Gercel-Taylor, C. (2008) MicroRNA signatures of tumor-derived exosomes as diagnostic biomarkers of ovarian cancer. *Gynecol. Oncol.* **110,** 13–21
27. Wang, K., Zhang, S., Weber, J., Baxter, D., and Galas, D. J. (2010) Export of microRNAs and microRNA-protective protein by mammalian cells. *Nucleic Acids Res.* **38,** 7248–7259
28. Will, C. L., Schneider, C., Hossbach, M., Urlaub, H., Rauhut, R., Elbashir, S., Tuschl, T., and Luhrmann, R. (2004) The human 18S U11/U12 snRNP contains a set of novel proteins not found in the U2-dependent spliceosome. *RNA* **10,** 929–941
29. Jang, M., Kim, S. S., and Lee, J. (2013) Cancer cell metabolism: implications for therapeutic targets. *Exp. Mol. Med.* **45,** e45
30. Currie, E., Schulze, A., Zechner, R., Walther, T. C., and Farese, R. V., Jr. (2013) Cellular fatty acid metabolism and cancer. *Cell Metab.* **18,** 153–161
31. Santos, C. R., and Schulze, A. (2012) Lipid metabolism in cancer. *FEBS J.* **279,** 2610–2623
32. Hartmann, D., Lucks, J., Fuchs, S., Schiffmann, S., Schreiber, Y., Ferreiros, N., Merkens, J., Marschalek, R., Geisslinger, G., and Grosch, S. (2012) Long chain ceramides and very long chain ceramides have opposite effects on human breast and colon cancer cell growth. *Int. J. Biochem. Cell Biol.* **44,** 620–628
33. Mills, G. B., and Moolenaar, W. H. (2003) The emerging role of lysophosphatidic acid in cancer. *Nat. Rev. Cancer* **3,** 582–591
34. Kuwata, S., Ohkubo, K., Kumamoto, S., Yamaguchi, N., Izuka, N., Murota, K., Tsujiuchi, T., Iwamori, M., and Fukushima, N. (2013) Extracellular lipid metabolism influences the survival of ovarian cancer cells. *Biochem. Biophys. Res. Commun.* **439,** 280–284
35. Oda, S. K., Strauch, P., Fujiwara, Y., Al-Shami, A., Oravecz, T., Tigyi, G., Pelanda, R., and Torres, R. M. (2013) Lysophosphatidic acid inhibits CD8 T cell activation and control of tumor progression. *Cancer Immunol. Res.* **1,** 245–255
36. Bian, S., Zhang, L., Duan, L., Wang, X., Min, Y., and Yu, H. (2013) Extracellular vesicles derived from human bone marrow mesenchymal stem cells promote angiogenesis in a rat myocardial infarction model. *J. Mol. Med*. **92,** 387–397

37. Leary, A., Auclin, E., Pautier, P., and Lhommé, C. (2013) *Ovarian Cancer—A Clinical and Translational Update*, InTech, Rijeka, Croatia
38. Quidville, V., Alsafadi, S., Goubar, A., Commo, F., Scott, V., Pioche-Durieu, C., Girault, I., Baconnais, S., Le Cam, E., Lazar, V., Delaloge, S., Saghatchian, M., Pautier, P., Morice, P., Dessen, P., Vagner, S., and Andre, F. (2013) Targeting the deregulated spliceosome core machinery in cancer cells triggers mTOR blockade and autophagy. *Cancer Res.* **73,** 2247–2258
39. Weber, J. A., Baxter, D. H., Zhang, S., Huang, D. Y., Huang, K. H., Lee, M. J., Galas, D. J., and Wang, K. (2010) The microRNA spectrum in 12 body fluids. *Clin. Chem.* **56,** 1733–1741
40. Arroyo, J. D., Chevillet, J. R., Kroh, E. M., Ruf, I. K., Pritchard, C. C., Gibson, D. F., Mitchell, P. S., Bennett, C. F., Pogosova-Agadjanyan, E. L., Stirewalt, D. L., Tait, J. F., and Tewari, M. (2011) Argonaute2 complexes carry a population of circulating microRNAs independent of vesicles in human plasma. *Proc. Natl. Acad. Sci. U.S.A.* **108,** 5003–5008
41. Turchinovich, A., Weiz, L., Langheinz, A., and Burwinkel, B. (2011) Characterization of extracellular circulating microRNA. *Nucleic Acids Res.* **39,** 7223–7233
42. Vickers, K. C., Palmisano, B. T., Shoucri, B. M., Shamburek, R. D., and Remaley, A. T. (2011) MicroRNAs are transported in plasma and delivered to recipient cells by high-density lipoproteins. *Nat. Cell Biol.* **13,** 423–433
43. Ladd, J. J., Chao, T., Johnson, M. M., Qiu, J., Chin, A., Israel, R., Pitteri, S. J., Mao, J., Wu, M., Amon, L. M., McIntosh, M., Li, C., Prentice, R., Disis, N., and Hanash, S. (2013) Autoantibody signatures involving glycolysis and splicesome proteins precede a diagnosis of breast cancer among postmenopausal women. *Cancer Res.* **73,** 1502–1513
44. Théry, C., Amigorena, S., Raposo, G., and Clayton, A. (2006) Isolation and characterization of exosomes from cell culture supernatants and biological fluids. *Curr. Protoc. Cell Biol.* Chapter 3:Unit 3 22
45. ASTM E2834-12, Standard Guide for Measurement of Particle Size Distribution of Nanomaterials in Suspension by Nanoparticle Tracking Analysis (NTA), ASTM International, West Conshohocken, PA, 2012, www.astm.org.